This article was downloaded by: [Siauliu University Library]
On: 17 February 2013, At: 07:27
Publisher: Taylor & Francis
Informa Ltd Registered in England and Wales Registered Number: 1072954
Registered office: Mortimer House, 37-41 Mortimer Street, London W1T 3JH, UK

Advanced Composite Materials
Publication details, including instructions for authors and subscription information:
http://www.tandfonline.com/loi/tacm20

On crashworthiness of FRP thin-walled circular tubes under dynamic axial compression

Yukinobu Uchikawa [a] , Masaaki Itabashi [b] & Kozo Kawata [c]

[a] Department of Materials Science and Technology, Faculty of Industrial Science and Technology, Science University of Tokyo, 2641, Yamazaki, Noda, Chiba 278, Japan

[b] Department of Materials Science and Technology, Faculty of Industrial Science and Technology, Science University of Tokyo, 2641, Yamazaki, Noda, Chiba 278, Japan

[c] Department of Materials Science and Technology, Faculty of Industrial Science and Technology, Science University of Tokyo, 2641, Yamazaki, Noda, Chiba 278, Japan

Version of record first published: 02 Apr 2012.

To cite this article: Yukinobu Uchikawa , Masaaki Itabashi & Kozo Kawata (1997): On crashworthiness of FRP thin-walled circular tubes under dynamic axial compression, Advanced Composite Materials, 6:3, 239-252

To link to this article: http://dx.doi.org/10.1163/156855197X00102

PLEASE SCROLL DOWN FOR ARTICLE

Full terms and conditions of use: http://www.tandfonline.com/page/terms-and-conditions

This article may be used for research, teaching, and private study purposes. Any substantial or systematic reproduction, redistribution, reselling, loan, sub-licensing, systematic supply, or distribution in any form to anyone is expressly forbidden.

The publisher does not give any warranty express or implied or make any representation that the contents will be complete or accurate or up to date. The accuracy of any instructions, formulae, and drug doses should be independently verified with primary sources. The publisher shall not be liable for any loss, actions, claims, proceedings, demand, or costs or damages whatsoever or howsoever caused arising directly or indirectly in connection with or arising out of the use of this material.

Downloaded by [Siauliu University Library] at 07:27 17 February 2013

Adv. Composite Mater., Vol. 6, No. 3, pp. 239–252 (1997)
© VSP 1997.

On crashworthiness of FRP thin-walled circular tubes under dynamic axial compression

YUKINOBU UCHIKAWA, MASAAKI ITABASHI and KOZO KAWATA

Department of Materials Science and Technology, Faculty of Industrial Science and Technology, Science University of Tokyo, 2641, Yamazaki, Noda, Chiba 278, Japan

Downloaded by [Siauliu University Library] at 07:27 17 February 2013

Received 14 June 1996; accepted 26 September 1996

Abstract—Dynamic crash behavior under dynamic axial compression of GFRP, CFRP and KFRP thin-walled circular tubes is reported. Such tubes may be used as structural members in fields where their light weight property is regarded as important. For precise characterization of dynamic properties, the KHKK 'one-bar method' [1] is applied. These materials are evaluated from the standpoint of crashworthiness (dynamic crash stress), and their individual characteristics, that arise from the composing fiber itself and from reinforcing fiber patterns with their varied fracture appearances, are clarified.

Keywords: mean crash stress; thin-walled circular tube; axial compression; crashworthiness.

1. INTRODUCTION

In recent years, a considerable amount of research has been undertaken on structural crashworthiness. For unsymmetric quasi-static buckling of PVC circular tubes, theoretical and experimental evaluations were done by Soden *et al.* [2]. Dynamic data were acquired for unsymmetric dynamic buckling of metallic thin-walled circular tubes under axial stress and the effects of materials and of radius-to-thickness ratio were obtained by Kawata *et al.* [3, 4]. The effect of matrix in energy absorption was studied for epoxy and PEEK composites by Hamada *et al.* [5].

In the present study, a series of experiments on dynamic crash stress under dynamic axial compression of FRP thin-walled circular tubes is undertaken. In the fields of transportation systems, for example, automobile and aerospace, structural design should be based upon mechanical properties, not only under quasi-static load but also under dynamic load. We consider a thin-walled circular FRP tube (reinforcing fiber: glass, carbon, or Kevlar) as the thin-walled structural element. By applying the dynamic properties characterization method based on the 'one-bar method', the crashworthiness under dynamic compression load can be evaluated. When the thin-walled circular tube is crashed by axial compression, the load rises sharply in the elastic area and then goes down, and then repeats the cyclic up and down behavior with the progress of the crash. The energy absorbed in the crash is acquired as an area under a load–displacement curve, but the elastic area is very small and its contribution is very little. So we deal with only the energy absorbed in the inelastic area, neglecting the elastic area. We define the mean plastic load over the elastic area as the 'mean crash load (MCL)'. Considering the dimensional difference in each FRP thin-walled circular tube made by hand lay-up, we define the 'mean crash stress (MCS)' as the MCL divided by the cross-sectional area of each specimen.

2. EXPERIMENTAL

2.1. Specimen

The following three type of materials are chosen:

(1) GFRP. Matrix: unsaturated polyester (Rigolac 158BQT).
Reinforcing fiber: E-glass (roving cloth: R-600; chopped strand mat: CM-450).

(2) CFRP. Matrix: epoxy (resin: ACR R97, hardener: ACR H4510).
Reinforcing fiber: Torayca T-300.

(3) KFRP. Matrix: epoxy (resin: ACR R97, hardener: ACR H4510).
Reinforcing fiber: Kevlar-49.

Six different types of thin-walled circular tubes were chosen (Table 1, Fig. 1). They consist of inner and outer layers of reinforcement, made by hand lay-up. The combinations of inner and outer layers are shown in Table 1. R means roving cloth, of which rovings are aligned 0° and 90° to the cylindrical axis. M means chopped strand mat with random fiber orientation. Thus, for example, M/R means the combination of inner M layer and outer R layer of the same thickness.

2.2. Principle of measurement for dynamic compression load–displacement relation [1]

For the analysis of the dynamic axial compressive behavior, it is important to measure exact crash load when the thin-walled circular tube is crashed under dynamic

Table 1.
Material type and composition of specimens

Material		GFRP				CFRP	KFRP
Composition		R/R	R/M	M/R	M/M	R/R	R/R
Layer	Inner	R	R	M	M	R	R
	Outer	R	M	R	M	R	R

R: Roving cloth (0°/90°).
M: Chopped strand mat.

Downloaded by [Siauliu University Library] at 07:27 17 February 2013

Downloaded by [Siauliu University Library] at 07:27 17 February 2013

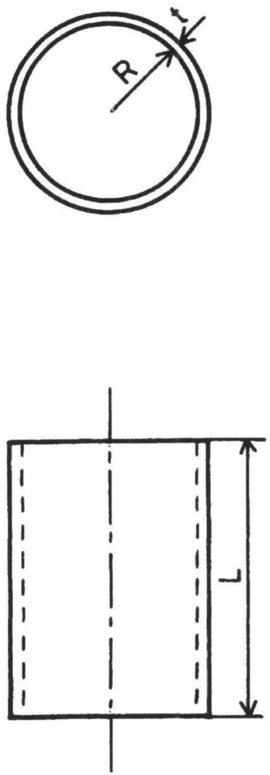

(Unit : mm)

Specimen	A	B	C	D	E	F
Material	GFRP				CFRP	KFRP
	R/R	R/M	M/R	M/M	R/R	R/R
Length L	45.0	45.1	48.6	49.1	44.7	44.7
Radius R	19.4	19.2	20.9	20.9	20.3	20.2
Thickness t	1.5	1.6	1.4	1.6	1.1	1.3
R/t ratio	13	12	16	13	18	16
V_f (%)	35	27	28	20	45	45

Figure 1. Specimen configuration.

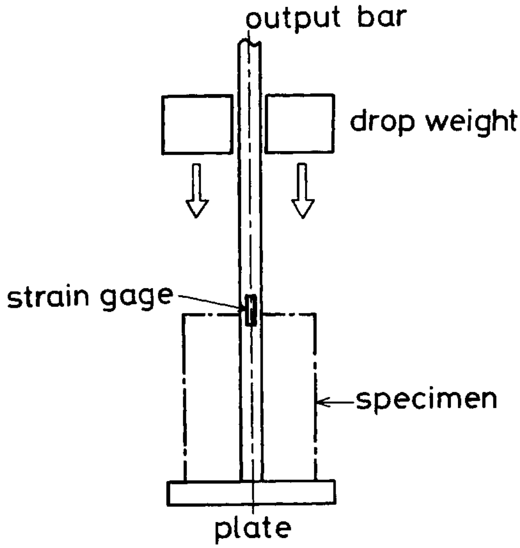

Figure 2. One-bar method for dynamic compression (block-to-bar type).

load. When the thin-walled circular tube deforms elastically or plastically by dynamic compression load, the variation of crash load with time propagates as a waveform. So we adopted the KHKK 'one-bar method' that can measure the dynamic load–displacement curve without reflected wave disturbance. This differs from measurement in a conventional system by using a load cell of short length. The theory of the one-bar method is explained in the following.

In Fig. 2, an output bar (304 stainless steel), of small diameter compared to its length, is hung from the upper fixing end. To the lower end of the bar, a stiff plate or flange is attached. The circular tube specimen is set on the plate. A drop weight (7.3 kg f, High carbon steel) is assumed as rigid in the theoretical treatment. When the weight falls on the specimen, the specimen is compressed dynamically and generates a compressive stress wave to the plate attached to the lower end of the output bar. This compressive stress wave gives a corresponding tensile stress wave to the output bar, due to the reflection at the free end. So the compressive load variation with time is detected as a tensile stress waveform by the strain gages (KYOWA, type KPS-2-E3) attached on the output bar. The effective measuring time is given by $2l/c$, where l is the distance between the gage station and the upper end of the bar and c is the longitudinal elastic wave velocity of the output bar. A vertical type high velocity loading system is shown in Fig. 3. The block diagram of measuring system is shown in Fig. 4. The quantities to be measured are load, axial displacement of the upper tube end (assuming that this is the same as the displacement of the weight) and velocity of the weight. The load is measured by the semiconductor strain gages cemented on the output bar at a-a′. This load $P(t)$ at time t is given as follows:

$$P(t) = S_0 E_b \varepsilon_g\left(t + \frac{a}{c}\right), \tag{1}$$

Downloaded by [Siauliu University Library] at 07:27 17 February 2013

Downloaded by [Siauliu University Library] at 07:27 17 February 2013

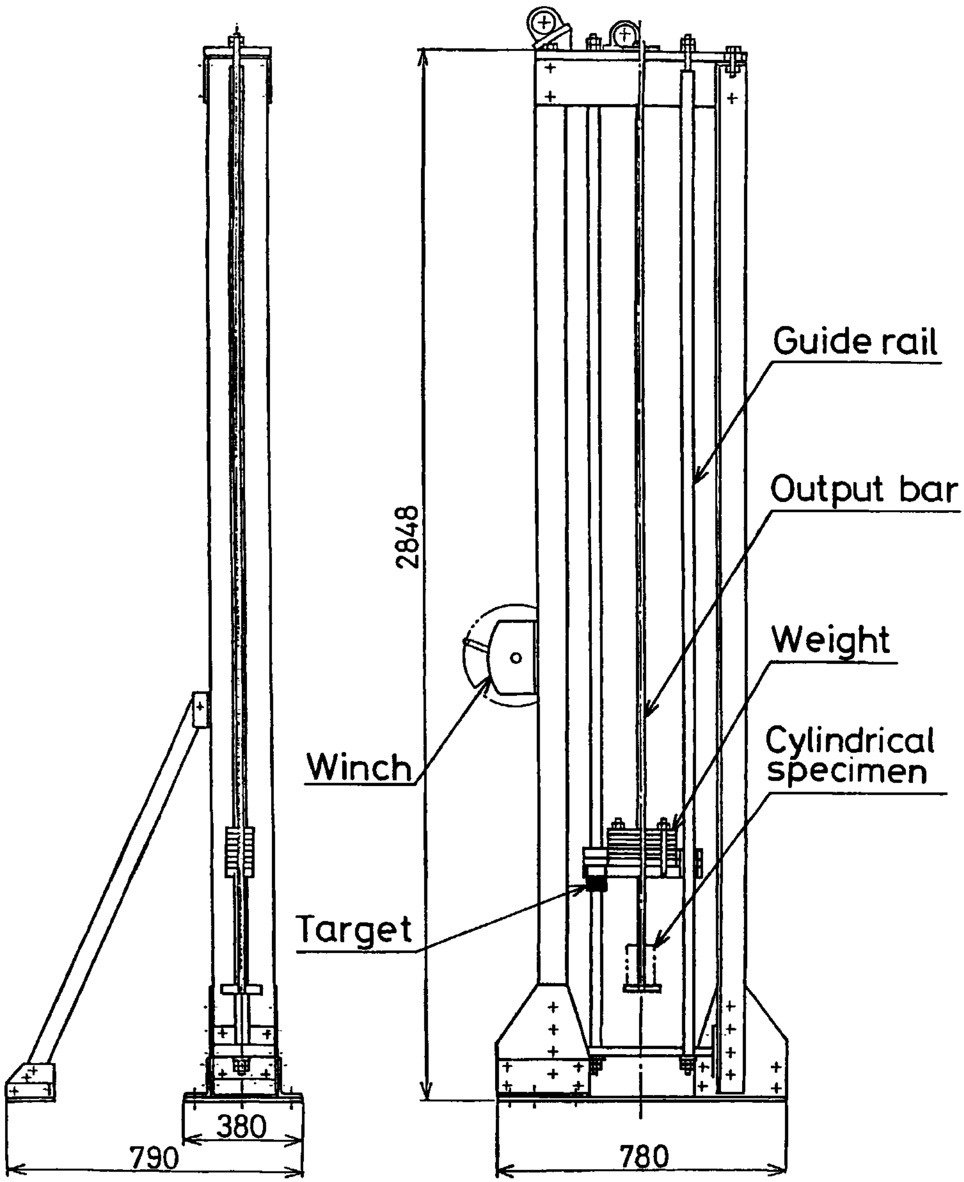

Figure 3. Dynamic compressive loading machine.

where S_0, E_b and c are the cross sectional area, Young's modulus and longitudinal elastic wave velocity, respectively, of the output bar, and $\varepsilon_g(t)$ is the strain of the output bar at the station situated at a distance a from the lower end of the output bar at time t counted from the beginning of impact. The displacement of the weight is measured using an electrooptical displacement transducer (Zimmer model 100D/II). From this displacement signal, by using a differentiator (Zimmer model 131c) in

Downloaded by [Siauliu University Library] at 07:27 17 February 2013

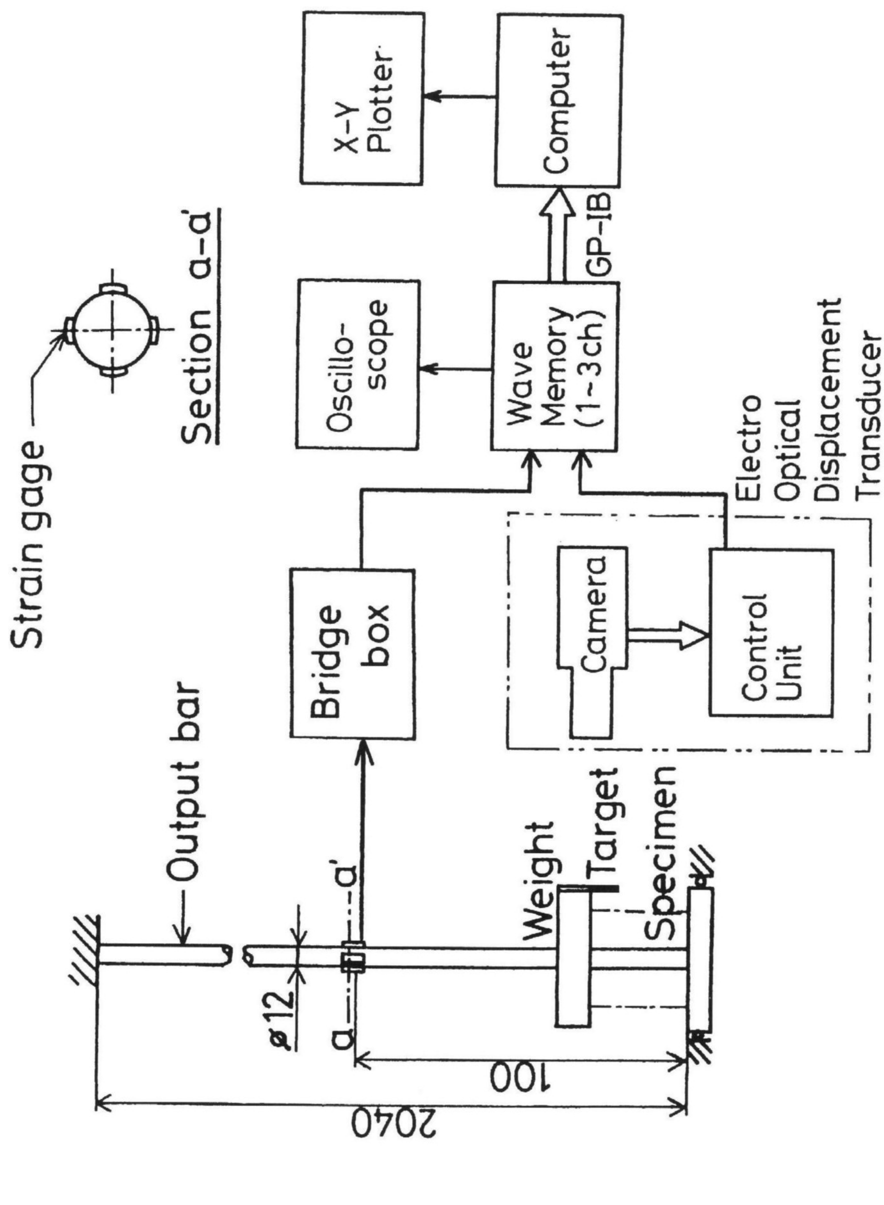

Figure 4. Block diagram of dynamic compressive load–displacement detection system.

the crash process, the velocity immediately after the beginning of the crash and mean velocity for the whole crash process, are obtained. The output signals of load, displacement and velocity are stored in three transient wave memories at the sampling frequency of 200 kHz and sent to a personal computer. The load–displacement curve is then drawn by an $X-Y$ plotter.

2.3. Velocity control in dynamic compression

For dynamic compression, the vertical type high velocity loading system (Fig. 3) based on the one-bar method is used. In this system, the specimen is given dynamic axial compression load by the free-falling weight. For higher velocity than the free fall, the weight is accelerated by rubber ropes. By this technique, the velocity of the weight can be changed from 3 to 10 m/s.

2.4. Quasi-static compression

For a quasi-static compression test, the specimen is given axial compression load by an universal material testing machine (SHIMADZU, Autograph AG10-TA) with the capacity of 98 kN and loading velocity of 0.05–500 mm/min. The quasi-static loading speed is set at 5 mm/min. We derive a quasi-static load–displacement curve for this velocity from the installed $X-Y$ recorder.

Downloaded by [Siauliu University Library] at 07:27 17 February 2013

3. RESULTS AND DISCUSSION

3.1. Results

Load–displacement curves for a GFRP(R/M) specimen under quasi-static and dynamic load are clearly obtained, as shown in Figs 5 and 6, respectively. In these figures, the MCL is shown by a chain line, excluding the elastic area.

3.1.1. Quasi-static load–displacement relations. In a typical example (Fig. 5), the specimen is GFRP(R/M) and the loading velocity is 5 mm/min. The load rises sharply up to the elastic buckling limit and decreases, but after that it repeats the cyclic up and down behavior with the progress of collapse. This tendency is common to all cases tested. The MCL is larger than the maximum load in the elastic area.

3.1.2. Dynamic load–displacement relations. In a typical example (Fig. 6), the specimen is GFRP(R/M) and the loading velocity of load is 5.7 m/s. In this case also, the load rises sharply to the elastic buckling load, then decreases, and further shows again the up and down behavior. The MCL is larger than the maximum load in the elastic area. For this case, the effective measuring time is 800 μs.

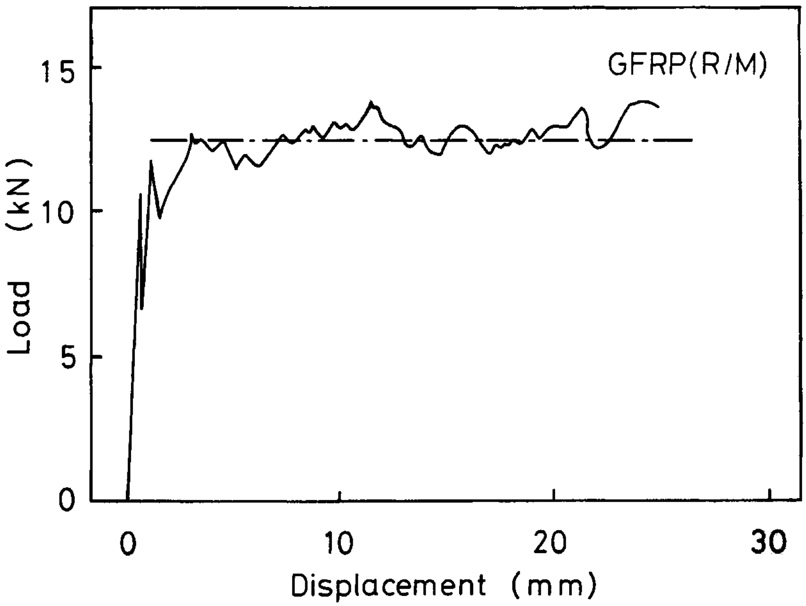

Figure 5. Quasi-static compressive load–displacement curve for GFRP(R/M) specimen ($V = 5$ mm/min).

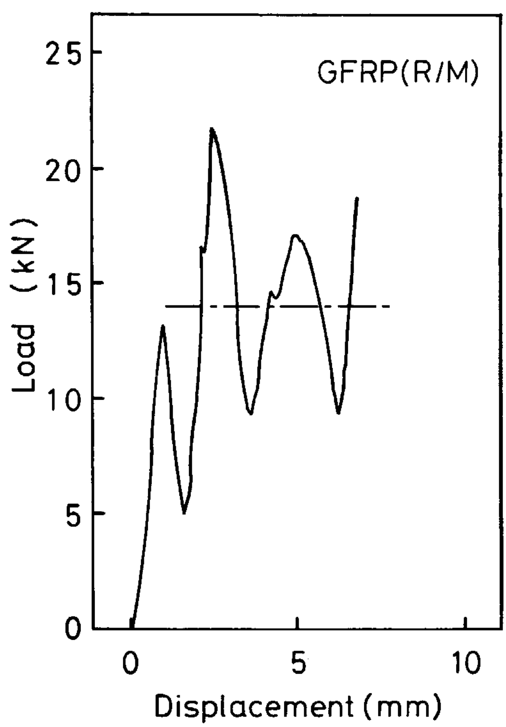

Figure 6. Dynamic compressive load–displacement curve for GFRP(R/M) specimen ($V = 5.7$ m/s).

Downloaded by [Siauliu University Library] at 07:27 17 February 2013

Downloaded by [Siauliu University Library] at 07:27 17 February 2013

3.2. Fracture appearance after collapse and related fracture mechanism of FRP thin-walled circular tubes

In Fig. 7, photographs showing fracture appearance of the GFRP, CFRP and KFRP thin-walled circular tubes under quasi-static and dynamic axial compression loads are shown. Figure 7(b), for GFRP(M/M), shows that fiber-reinforced layers are peeled off to inner and outer sides of the tube individually, curled to both sides, under both quasi-static and dynamic loads and matrix resin is fragmented into very small pieces, remarkably under dynamic load rather than under quasi-static load. In Figure 7(a), for GFRP(R/R), and 7(b), the effects of different fiber reinforcing orientation can be obtained. In Figure 7(a), (c) and (d), the fiber reinforcing pattern of R/R is common for these specimens. Figure 7(c), for CFRP(R/R), shows that, under quasi-static load, ideal peeling and curling style of collapse is seen, as for GFRP(M/M). But under dynamic load, there is no delamination. Ring generation mode is predominant. The width of the rings is comparable to that of the roving. In Fig. 7(d), for KFRP(R/R), it is observed that there is no delamination and the specimen forms diamond patterns composed of plastic hinges, regardless of the loading velocity. This collapse mode is familiar for the collapse of metallic tubes.

From the standpoint of the mechanism of energy absorption, in the GFRP thin-walled circular tube, under both quasi-static and dynamic loads, delamination, minute breakage of matrix and fiber breakage of roving width scale are the main factors. This observed crash style—successive peeling of inner and outer layers from the loaded end of the circular tube and their curling out to both outsides from the laid-up face—is an interesting characteristic of the FRP tubes. In CFRP under quasi-static load, the mechanism is similar to that for GFRP. But under dynamic load, it shows a completely different style of collapse, namely, it is split into the circular rings. This phenomenon seems to arise because the circular CFRP rovings limit the freedom of expansion in the circular direction, so that such fracture may be generated in axial rovings at intervals of the width of circular rovings. In KFRP under both quasi-static and dynamic loads, energy absorption is achieved by progress of a plastic hinge, as in metallic thin-walled circular tubes [3, 4]. So, it is found that the style of collapse is different for different types of reinforcing fiber. Further, it is noteworthy that the style of collapse of CFRP(R/R) under quasi-static load does not show the style of GFRP(R/R) but that of GFRP(M/M).

3.3. Velocity dependence of mean crash stress

In Figs 8a–8c, the relation between mean crash stress (MCS) and velocity for GFRP(R/R, M/M); GFRP(R/M, M/R); and GFRP(R/R), CFRP(R/R), KFRP(R/R) are shown, respectively. From Figs 8a and 8b, it may be seen that MCS increases almost linearly with increasing velocity for GFRP, that is, it shows positive crashing velocity dependence (increasing rate of MCS with increasing velocity). The rate of increase and strength under quasi-static load vary with the pattern of fiber orientation. Under quasi-static load, (R/R) is smaller than the others and the rate of increase of (M/R) is larger than the others. In Fig. 8c, showing the velocity

Quasi-static Dynamic

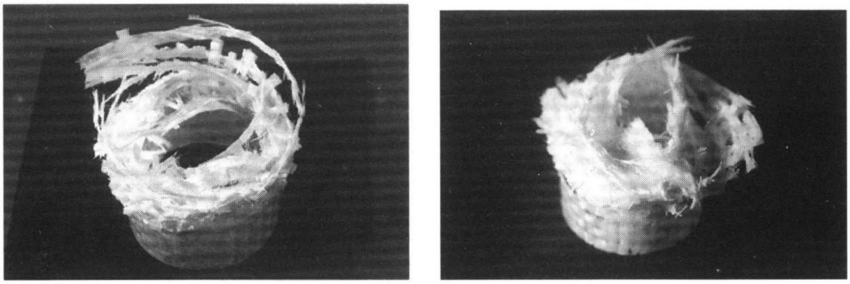

(a)

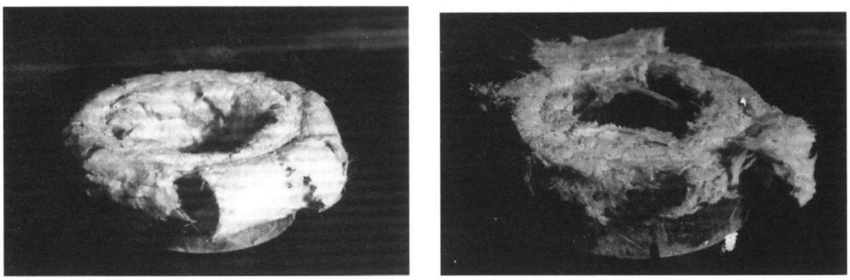

(b)

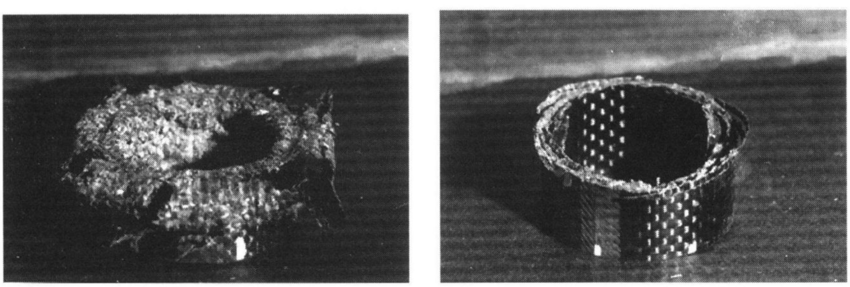

(c)

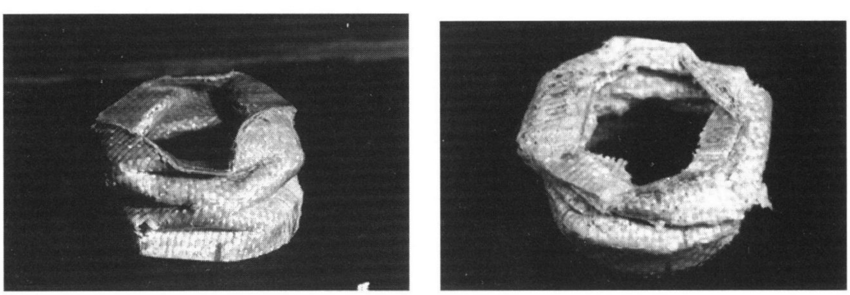

(d)

Figure 7. Fracture appearance of FRP circular tubes; (a) GFRP(R/R); (b) GFRP(M/M); (c) CFRP(R/R); (d) KFRP(R/R).

Downloaded by [Siauliu University Library] at 07:27 17 February 2013

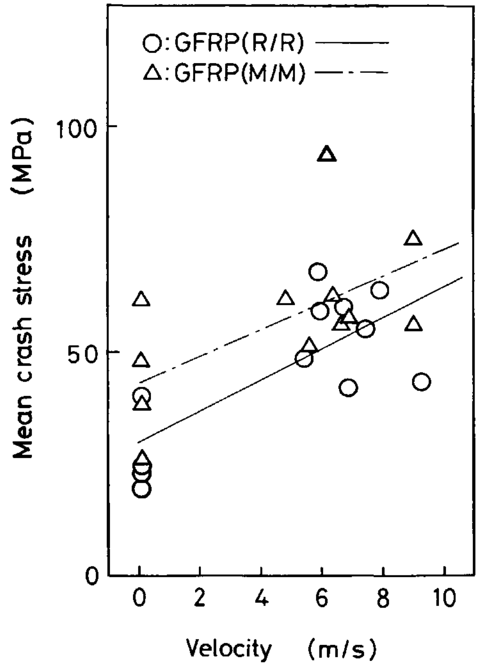

Figure 8a. Experimental results of mean crash stress–velocity relations for GFRP(R/R, M/M).

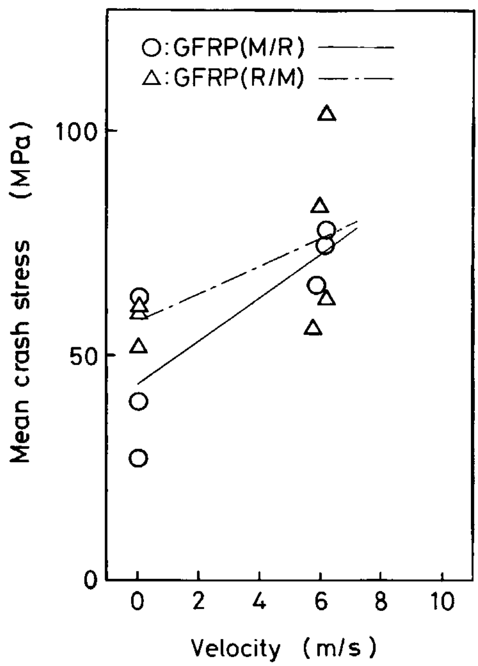

Figure 8b. Experimental results of mean crash stress–velocity relations for GFRP(M/R, R/M).

Downloaded by [Siauliu University Library] at 07:27 17 February 2013

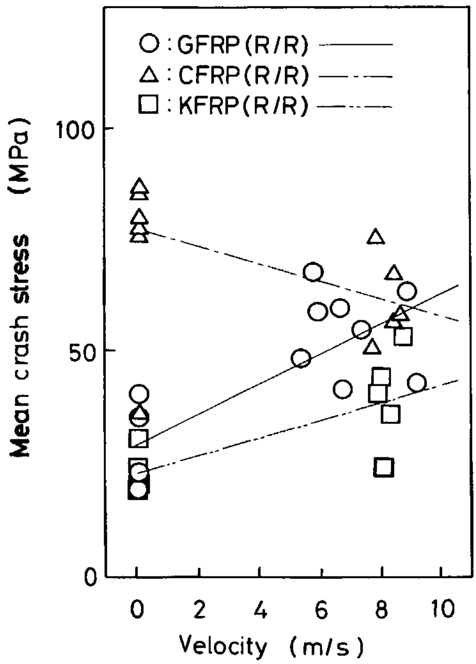

Figure 8c. Experimental results of mean crash stress–velocity relations for GFRP(R/R), CFRP(R/R) and KFRP(R/R).

dependence of MCS for GFRP, CFRP, and KFRP with the same reinforcing pattern (R/R), it is seen that there is a remarkable effect of the reinforcing fibers. It should be noted that the velocity dependence takes a negative value in CFRP, differing from GFRP and KFRP. From our former experiments with metallic thin-walled circular tubes [3, 4], it is known that for mild steel tubes, the velocity dependence of mean crash load is positive, but for Al alloy tubes, the dependence is nearly equal to zero. So, we can say that in the FRP thin-walled circular tubes, the velocity dependence is a special feature of FRP, differing clearly from metals.

3.4. Effects of fiber orientation patterns in crashworthiness of FRP thin-walled circular tube

When we consider the light weight property and crash safety of structures, the absorbed energy per unit weight of each material is one of the most important factors. An index of crashworthiness, which is the MCS divided by density, is taken. The value, its increment and dependence of MCS/ρ with respect to the loading velocity are shown in Table 2. Under quasi-static load, CFRP(R/R) indicates strikingly larger MCS/ρ than the others. Under dynamic load, GFRP(R/M, M/R, M/M) and CFRP(R/R) show relatively larger MCS/ρ values. The dependence for GFRP(M/R) is the largest. In six types of tubes tested, only CFRP(R/R) shows negative increment and dependence.

Downloaded by [Siauliu University Library] at 07:27 17 February 2013

Table 2.
Specific mean crash stress of FRP thin-walled circular tubes and their velocity dependence

Specimen		GFRP				CFRP	KFRP
		R/R	R/M	M/R	M/M	R/R	R/R
MCS[a]/ρ (10^2 m)	Quasi-static	19.4	35.6	30.4	33.3	62.1	20.3
	Dynamic	31.3	50.6	49.4	48.3	47.6	35.5
Increment (%)[b]		61	42	63	45	−23	75
Dependence (10^2 m s/m)[c]		1.7	2.4	3.1	2.2	−1.7	1.8

[a] MCS: mean crash stress.
[b] Increment = $\frac{D-S}{S} \times 100$ (%), D, S: dynamic and static values of MCS/ρ respectively.
[c] Dependence = $\frac{\mathrm{d(MCS}/\rho)}{\mathrm{d}V}$.

Furthermore, in a comparison of four patterns of the GFRP, the following should be noted:
1) In R/R *vs.* M/M, the latter shows higher MCS/ρ both in quasi-static and in dynamic load.
2) In R/M *vs.* M/R, the former shows higher MCS/ρ both in quasi-static and in dynamic load.
3) In four patterns of the GFRP, the highest MCS/ρ both in quasi-static and in dynamic loading is R/M.
4) When M is combined, in any form, the value becomes higher compared with R/R.

4. CONCLUSIONS

From the series of experiments on FRP thin-walled circular tubes of six types described above: four types (R/R, R/M, M/R, M/M) of the GFRP, and the R/R type of CFRP and KFRP, the following facts have emerged.

1. For FRP thin-walled circular tubes, the mean crash stress under dynamic axial compression load is well characterized by the one-bar method.
2. Velocity dependence of MCS is positive for GFRP of four types (R/R, R/M, M/R, M/M) and for KFRP(R/R). On the other hand, it is negative for CFRP(R/R).
3. The effects of fiber orientation pattern and of the nature of the fiber itself in MCS/ρ (specific MCS, ρ: weight per unit volume) is remarkable, for both quasi-static and dynamic conditions.
   3.1. In comparison among four types of GFRP, the maximum dynamic MCS/ρ is obtained for R/M.
   3.2. In R/R for GFRP, CFRP and KFRP, the order of MCS/ρ is CFRP > KFRP > GFRP in both static and dynamic conditions.
   3.3. The GFRP thin-walled circular tubes of R/M, M/R and M/M—that is, including M—are excellent on crashworthiness under dynamic conditions. In CFRP thin-walled circular tube, its static value is higher than the other FRP but the dynamic value is a little smaller than the CFRP specimen including M.

Downloaded by [Siauliu University Library] at 07:27 17 February 2013

4. The characteristic fracture appearance of FRP thin-walled circular tube under static and dynamic compression is similar to that with a metallic specimen.

   4.1. In GFRP (static, dynamic) and CFRP (static), successive peeling of outer and inner layers and curling to the respective sides, is observed.

   4.2. In CFRP (dynamic), fracture to ring-like pieces is observed.

   4.3. In KFRP, collapse similar to that with metallic specimens, that is, plastic collapse with diamond patterns composed of plastic hinges, is observed.

5. If thin-walled circular tube is used as a structural member with impact absorbing ability, then in order to obtain high crashworthiness it is recommended that materials of which static MCS/ρ and proportional dependence of MCS/ρ with respect to velocity are positive and large, respectively, should be used.

Downloaded by [Siauliu University Library] at 07:27 17 February 2013

Acknowledgements

The authors express their hearty thanks to Professor Hiroshi Fukuda, Science University of Tokyo, for his kind discussion and comments, to DJK Research Center Inc. for the supply of suitable FRP specimens, and to Messrs. Masato Akiyama, Masaki Nakajima and Toshiyuki Higuchi for their eager help in carrying out the series of experiments.

REFERENCES

1. Kawata, K., Hashimoto, S., Kurokawa, K. and Kanayama, N. A new testing method for the characterization of materials in high velocity tension. In: *Mechanical Properties at High Rates of Strain 1979*, Harding, J. (Ed.). Inst. of Phys., Conf. Ser. No. 47, Bristol and London (1979), pp. 71–80.
2. Soden, P. D., Al-Hassani, S. T. S. and Johnson, W. The crumpling of polyvinylchloride tubes under static and dynamic axial loads. In: *Mechanical Properties at High Rates of Strain 1974*, Harding, J. (Ed.). Inst. of Phys., Conf. Ser. No. 21, London and Bristol (1974), pp. 327–338.
3. Kawata, K., Miyamoto, I. and Minamitani, R. Plastic collapse in dynamic axial compression of thin-walled circular tube. In: *Proc. International Symposium on Intense. Dynamic Loading and Its Effects*. Science Press, Beijing (1986), pp. 454–458.
4. Kawata, K., Matsumoto, S. and Yoshimizu, E. On the effects of materials and radius to thickness ratio in dynamic plastic buckling of circular tubes under axial impact. In: *Mechanical Properties of Materials at High Rates of Strain 1989*, Harding, J. (Ed.). Inst. of Phys., Conf. Ser. No. 102, Oxford, Bristol (1989), pp. 465–472.
5. Hamada, H., Coppola, J. C., Hull, D., Maekawa, Z. and Sato, H. Comparison of energy absorption of carbon/epoxy and carbon/PEEK composite tubes. *Composites* **23**, 245–252 (1992).